Cellulose (2014) 21:3781–3795
DOI 10.1007/s10570-014-0373-5

ORIGINAL PAPER

In situ photoreduction of Ag^+-ions by TiO_2 nanoparticles deposited on cotton and cotton/PET fabrics

Milica Milošević · Marija Radoičić · Zoran Šaponjić · Tim Nunney · Christopher Deeks · Vesna Lazić · Miodrag Mitrić · Tamara Radetić · Maja Radetić

Received: 20 May 2014 / Accepted: 22 July 2014 / Published online: 1 August 2014
© Springer Science+Business Media Dordrecht 2014

Abstract The possibility of in situ photoreduction of Ag^+-ions using TiO_2 nanoparticles deposited on cotton and cotton/PET fabrics in the presence of amino acid alanine and methyl alcohol has been discussed. The possible interaction between TiO_2, alanine and Ag^+-ions was evaluated by FTIR analysis. The fabrication of TiO_2/Ag nanoparticles on both fabrics was confirmed by SEM, EDX, XRD, XPS and AAS analyses. Cotton and cotton/PET fabrics impregnated with TiO_2/Ag nanoparticles provided maximum reduction of Gram-negative bacteria *Escherichia coli* and Gram-positive bacteria *Staphylococcus aureus*. Although excellent antibacterial activity was preserved after ten washing cycles, a significant amount of silver leached out from the fabrics into the washing bath. The perspiration fastness assessment revealed that smaller amounts of silver were also released from the fabrics into artificial sweat at pH 5.50 and 8.00. In addition, deposited TiO_2/Ag nanoparticles imparted maximum UV protection to fabrics.

Keywords TiO_2 nanoparticles · Ag nanoparticles · Photoreduction · Antibacterial activity · UV protection

M. Milošević · M. Radoičić · Z. Šaponjić · M. Mitrić
Vinča Institute of Nuclear Sciences, University of Belgrade, Belgrade, Serbia

T. Nunney · C. Deeks
Thermo Fisher Scientific, West Sussex, UK

V. Lazić
Innovation Center of the Faculty of Technology and Metallurgy, University of Belgrade, Belgrade, Serbia

T. Radetić · M. Radetić (✉)
Faculty of Technology and Metallurgy, University of Belgrade, Belgrade, Serbia
e-mail: maja@tmf.bg.ac.rs

Introduction

The antimicrobial finishing of textile materials with silver nanoparticles (Ag NPs) has been extensively studied over the last decade (Lee et al. 2003; Yuranova et al. 2003; Lee and Jeong 2005; Gorenšek and Recelj 2007; Vigneshwaran et al. 2007; Pohle et al. 2007; Radetić et al. 2008; Ilić et al. 2009; Kelly and Johnston 2011; El-Shishtawy et al. 2011; Gorjanc et al. 2012; Tang et al. 2013; Nam and Condon 2014). Although numerous finishing procedures have been developed, the most of them are based on dip-coating of fabrics with colloidal Ag NPs (Radetić 2013). The conventional routs for the synthesis of colloidal Ag NPs usually involve various reducing agents and organic compounds which control the formation, size, shape and stability of Ag NPs (Messaoud et al. 2010). In addition to their potentially undesirable environmental impact, these organic compounds may diminish or even inhibit the antimicrobial action of Ag NPs. In order to avoid the use of strong reducing agents and stabilizers, we have proposed different approach that

relies on in situ generation of Ag NPs by photoreduction of Ag^+-ions from the solution in the presence of amino acid alanine and methyl alcohol on the surface of TiO_2 NPs deposited on polyester (PET) fabric (Milošević et al. 2013a).

Namely, the surface modification of TiO_2 NPs smaller than 20 nm with amino acid alanine leads to a replacement of TiO_2 surface hydroxyl groups and coordination of surface Ti atoms with carboxyl groups which simultaneously bind Ag^+-ions (Rajh et al. 1996, 1998). Therefore, enhanced adsorption of Ag^+-ions before illumination can be expected. The exposure of TiO_2 to UV light with an energy that matches or exceeds its band gap results in a generation of electron/hole pairs. They can further take part in different oxidation and reduction processes on the particle surface. However, the high rate of their recombination emerges as a major limitation of TiO_2 NPs. Surface modification of TiO_2 NPs with amino acids also results in increased charge separation and thus, enhanced photocatalytic activity of photogenerated electrons (Rajh et al. 1996, 1998).

Methyl alcohol has been used as an efficient hole-scavenger ($E°–(CH_3OH/^{\cdot}CH_2OH) = +1.2$ V) that eventually ensures an increase of the yield of the trapped electrons (Stockhausen and Henglein 1971). Previous studies demonstrated that electrochemical oxidation of methyl alcohol brings about the formation of the electron-donating methanol radical ($E°(^{\cdot}CH_2–OH/CH_2O) = -0.95$ V) (Breitenkamp et al. 1976). The net effect is that from one photon of absorbed light two electrons are generated. This phenomenon known as a current-doubling effect induces improved photoreduction rate of Ag^+-ions (Nogami and Kennedy 1989). Taking into account the redox potential of methanol radical ($^{\cdot}CH_2OH$, -0.95 V), it can be anticipated that it is capable to reduce Ag^+-ions as well.

Reported results showed that fabricated TiO_2/Ag NPs imparted extraordinary antimicrobial properties to PET fabrics (Milošević et al. 2013a). Maximum microbial reduction was preserved after ten washing cycles indicating excellent washing fastness. Encouraging results motivated us to continue the research on cotton and cotton/PET fabrics. Initially, the same procedure has been performed to cotton fabric. Although large amount of TiO_2/Ag NPs has been generated on the surface of cotton fabric and desired level of antibacterial activity has been achieved (Milošević et al. 2013b), the mechanical properties of the fabric were deteriorated. Unlike PET fibers, cotton fibers are prone to hydrolysis in acidic conditions. Low pH and elevated temperature during the treatment resulted in deterioration of the fabric strength. We had to go step further and adjust the existing procedure to cotton fibers. In adjusted procedure, the duration of dip-coating process with TiO_2 NPs and photoreduction were shortened whereas the curing of fabric after dip-coating in TiO_2 NPs colloidal solution was omitted. The impregnation of cotton and cotton/PET fabrics with TiO_2/Ag NPs produced in accordance with adjusted procedure caused certain morphological and chemical changes that were evaluated by SEM, EDX, XRD and XPS, respectively. Antibacterial activity of deposited TiO_2/Ag NPs was tested against Gram-negative bacteria *E. coli* and Gram-positive bacteria *S. aureus*.

Experimental

Materials

Desized and bleached cotton (Co, 168 g/m^2) and cotton/PET (Co/PET, 65/35, 196 g/m^2) woven fabrics were used as substrates in this study. In order to remove surface impurities, the fabrics were cleaned in the bath containing 0.5 % nonionic washing agent Felosan RG-N (Bezema) based on fatty alcohol ethoxylates at liquor-to-fabric ratio of 50:1. After 15 min of washing at 50 °C, the fabrics were rinsed once with warm water (50 °C) for 3 min and three times (3 min) with cold water. Subsequently, the fabrics were dried at room temperature.

A colloid consisting of TiO_2 NPs was synthesized by acidic hydrolysis of $TiCl_4$ in a manner analogous to the one proposed by Rajh et al. (1998). All chemicals used in the synthesis of colloid were of analytical grade (Aldrich, Fluka) and were used as received without any further purification. Milli-Q deionized water was used as a solvent. The solution of $TiCl_4$ cooled down to −20 °C was added drop-wise to cooled water (at 4 °C) under vigorous stirring and kept at this temperature in the next 30 min. The pH of the solution ranged between 0 and 1, depending on the concentration of $TiCl_4$. Slow growth of the particles was achieved by dialysis against water at 4 °C until the

pH of the solution reached 3.5. The concentration of TiO_2 colloid was determined from the concentration of the peroxide complex obtained after dissolving the particles in concentrated H_2SO_4 (Thompson 1984). In order to improve the crystallinity and overall photocatalytic efficiency of generated TiO_2 NPs, the colloid was thermally treated in reflux at 60 °C for 16 h (Mihailović et al. 2011). Mostly single crystalline, irregularly shaped TiO_2 NPs with average dimensions of 6 nm were observed by HREM (Mihailović et al. 2011). The electron diffraction pattern and Raman spectroscopy measurements confirmed the formation of anatase crystal structure (Mihailović et al. 2010).

Initially, a 1.00 g of Co fabric was immersed into 30 mL of 0.1 M TiO_2 colloid for 30 min and after squeezing at a pressure of 2 kg/cm^2, the sample was dried at room temperature. After 30 min of curing at 100 °C, dry fabric was rinsed twice (5 min) with deionized water and dried again at room temperature.

In situ photoreduction of Ag^+-ions on Co fabrics impregnated with TiO_2 NPs was carried out in accordance with the following procedure. A 0.1333 g of alanine was dissolved in 40 mL of water. The fabric coated with TiO_2 NPs was immersed in this solution for 10 min. 1.5 mL of $AgNO_3$ ($C = 0.015$ mol/L) and 0.4 mL of methyl alcohol were added into 58 mL of 1×10^{-3} M solution of HNO_3 (pH 3). This solution was added to alanine solution and mixed. Beaker was covered with quartz glass disc and sealed with parafilm. Teflon hose was inserted through the small hole and the system was purged in argon for 30 min. Subsequently, the system was illuminated with ULTRA-VITALUX lamp (300 W, Osram) for 30 min also in a stream of argon. The applied lamp provides sun-like irradiation. The fabric was removed from the solution, dried at room temperature, rinsed in Milli-Q deionized water for 15 min and again dried at room temperature.

Methods

FESEM

The morphology of the Co fibers was analyzed by field emission scanning electron microscopy (FESEM, Mira3 Tescan). The samples were coated with a thin layer of Au/Pd (85/15) prior to analysis.

EDX

Energy dispersive X-ray spectroscopy measurements (EDX) were carried out by scanning electron microscope JEOL JSM–6610LV. Gold layer was deposited on the samples before the analysis.

XRD

The XRD powder patterns were obtained using a Philips PW 1050 powder diffractometer with Ni-filtered Cu-K_λ radiation ($\lambda = 1.5418$ Å). The diffraction intensity was measured by the scanning technique (a step size of 0.05° and a counting time of 50 s per step).

XPS

X-ray photoelectron spectroscopy (XPS) measurements were performed in order to evaluate the chemistry and bonding variations of the Co and Co/PET fabrics. The XPS analysis was carried out using a K-Alpha spectrometer (Thermo Scientific, UK) utilizing a monochromated Al Kα ($h\nu = 1{,}486.6$ eV) X-ray source. The system base pressure was $<5 \times 10^{-9}$ mbar, however the pressure in the chamber during analysis was 2×10^{-7} mbar due to use of the charge neutralization system which employs a combination of low energy electrons and low energy argon ions to compensate for the loss of photoelectrons from an insulating sample. First, point analysis was carried out on all samples to determine their chemical composition. Maps were then acquired of all samples to determine the average composition of the surface.

AAS

The total content of Ag in the Co and Co/PET fabrics was determined using a Spectra AA 55 B (Varian) atomic absorption spectrometer (AAS).

FTIR

FTIR measurements were carried out in order to define binding structure of alanine modified TiO_2 nanoparticles and Ag^+- ions. Powdered samples for FTIR measurements were prepared by vacuum drying of solution of 0.04 M alanine and 0.04 M $AgNO_3$ (pH 3); colloidal dispersions of 0.08 M TiO_2, 0.04 M alanine (pH 3), and colloidal dispersions of 0.08 M TiO_2,

0.04 M alanine and 0.04 M $AgNO_3$ (pH 3). Powdered samples were mixed with potassium bromide (KBr, Sigma–Aldrich, Germany) in the ratio of 1:100, and then compressed to obtain KBr pellets. FTIR spectra were recorded, using Bomem MB 100 FTIR spectrophotometer, in the range of 400–4,000 cm^{-1}, with resolution of 4 cm^{-1}.

Antibacterial test

The antibacterial activity of fabrics was accomplished against Gram-negative bacteria *E. coli* ATCC 25922 and Gram-positive bacteria *S. aureus* ATCC 25923 using the standard test method for determining the antimicrobial activity of immobilized antimicrobial agents under dynamic contact conditions ASTM E 2149-01 (2001). The percentage of bacterial reduction (R, %) was calculated by the following equation:

$$R = \frac{C_0 - C}{C_0} \times 100 \quad (1)$$

where C_0 (CFU—colony forming units) is the number of bacteria colonies on the control fabric (untreated fabric without TiO_2/Ag NPs) and C (CFU) is the number of bacteria colonies on the fabric loaded with TiO_2/Ag NPs.

Washing fastness test

Washing fastness of fabrics impregnated with TiO_2/Ag NPs was examined after ten washing cycles in Polycolor (Werner Mathis AG) laboratory beaker dyer at 45 rpm. The fabrics were washed in the bath containing 5 g/L SDC standard detergent and 2 g/L Na_2CO_3 at liquor-to-fabric ratio of 80:1. After 50 min of washing at 95 °C (Co fabrics) and 35 min of washing at 40 °C (Co/PET fabrics), the fabrics were soaked twice in cold distilled water. The samples were then held under the tap water for 10 min, squeezed and dried at 70 °C. The percentage of microbial reduction after ten washing cycles was calculated according to Eq. (1). The concentration of silver which leached out from the fabrics into washing bath after each washing cycle was measured by AAS.

Perspiration fastness test

The perspiration fastness of fabrics was studied in artificial sweat at pH 5.5 and 8.0 that were prepared according to ISO 105-E04:1989E: Colour fastness to perspiration (1989). A 1 L of acidic artificial sweat (pH 5.5) contained: 0.5 g of L-histidine monohydrochloride monohydrate, 5 g of sodium chloride and 2.2 g of sodium dihydrogen orthophosphate dihydrate. A 1 L of alkaline artificial sweat (pH 8.0) contained: 0.5 g of L-histidine monohydrochloride monohydrate, 5 g of sodium chloride and 5 g of disodium hydrogen orthophosphate dodecahydrate. The solutions were adjusted to pH 5.5 and 8.0 with 0.1 M solution of sodium hydroxide. A 0.300 g of fabric was dipped into the artificial sweat at liquor-to-fabric ratio 50:1. The samples have been incubated in a water bath at 37 °C for 24 h. Afterwards the artificial sweat was collected and the concentration of released silver was measured by AAS.

UV protection

Transmission spectra of the samples were measured by UV–Vis spectrophotometer Varian Cary 100 Scan (Varian). The UV protection factor (UPF) values were automatically calculated on the basis of the recorded data in accordance with Australia/New Zealand standard AS/NZS 4399:1996 using a Startek UV fabric protection application software version 3.0 (Startek Technology).

Results and discussion

Impregnation of Co fabric with TiO_2/Ag NPs according to procedure developed for PET fabrics

The dip-coating procedure described in experimental section was initially developed for PET fabrics (Milošević et al. 2013a) and it was applied for the deposition of TiO_2 NPs on Co fabrics prior to photoreduction process. After in situ photoreduction of Ag^+-ions, the color of Co fabric turned from white to dark yellow. Evident color change indicated the presence of Ag NPs which was confirmed by FESEM analysis. Figure 1 shows a large amount of TiO_2/Ag NPs evenly deposited over the Co fiber surface. Obviously, narrow size distribution of fabricated TiO_2/Ag NPs with an average size of approximately 70 nm was obtained.

AAS measurements revealed that one gram of Co fabric contains 448.5 μg of Ag. This amount was almost

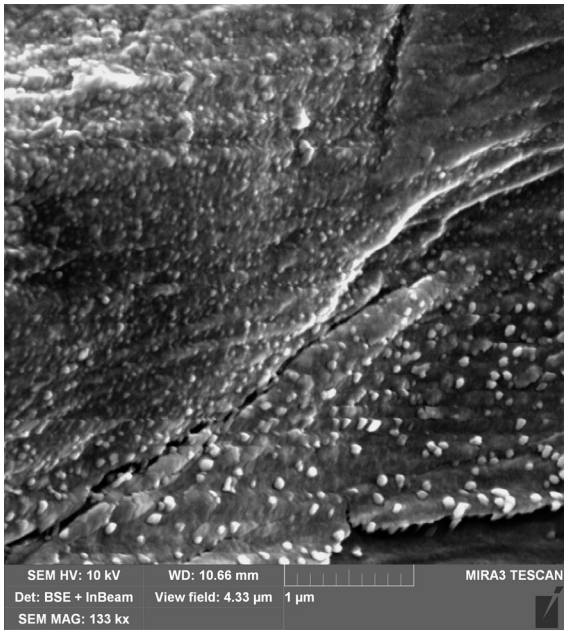

Fig. 1 FESEM image of pristine Co fiber impregnated with TiO_2/Ag NPs synthesized by procedure developed for PET fabric

three times larger compared to one detected in the PET fabric modified in the same manner (Milošević et al. 2013a). Huge amount of deposited TiO_2/Ag NPs was reflected in excellent antibacterial properties of Co fabric which were tested against bacteria *E. coli* and *S. aureus* (Milošević et al. 2013b). However, the deterioration of Co fabric strength appeared here as a major limitation due to hydrolysis of Co fibers in acidic conditions. In our experiments, Co fabrics were dip-coated in TiO_2 NPs colloid at pH 3.5 for 30 min and subsequently cured at 100 °C for 30 min. Low pH and elevated temperature resulted in weakening of the fabric mechanical properties. Co fabrics became so fragile that they could be manually torn without considerable effort. This became particularly obvious after washing likely because of the additional mechanical agitation. Such behavior of Co fabrics during the treatment with colloidal TiO_2 NPs in acidic conditions has been already reported in literature (Daoud et al. 2005).

Obtained results indicated that procedure initially developed for the modification of PET fabrics was not suitable for Co fabrics and it required revision. Therefore, in order to preserve both, desired antibacterial activity and mechanical properties, the duration of dip-coating process with TiO_2 NPs was cut down to 5 min, photoreduction process to 10 min whereas the curing of fabric after dip-coating in TiO_2 NPs colloid was omitted. Modified procedure was utilized for the treatment of Co and Co/PET fabrics which were further characterized.

Characterization of cotton and cotton/PET fabrics impregnated with TiO_2/Ag NPs

Successful fabrication of metallic Ag on Co and Co/PET fabrics by in situ photoreduction of Ag^+-ions using TiO_2 NPs was proved by XRD measurements. The XRD spectra of Co, Co + TiO_2/Ag, Co/PET and Co/PET + TiO_2/Ag samples are shown in Fig. 2. The diffraction peaks at $2\theta = 34.4°$ and 42.3° and broad peak at $2\theta \sim 46°$ in all XRD spectra are characteristic for Co fabrics (Yin et al. 2007).

The presence of face centered cubic (fcc) Ag metal phase in Co + TiO_2/Ag and Co/PET + TiO_2/Ag samples is confirmed by peaks that appeared at $2\theta = 38.4°$ in both XRD spectra, and correspond to (111) crystal plane (Zhong-Ai et al. 2010; Krklješ et al. 2007).

The changes in chemical composition of Co and Co/PET fibers caused by deposition of TiO_2/Ag NPs were evaluated by XPS measurements. In order to determine an average chemical composition of the fiber surface, each sample was mapped and representative high resolution spectra were collected. High resolution scans of Co and Co/PET fabrics in C1s region are shown in Fig. 3. High resolution scans accomplished in C1s, O1s, Ti2p and Ag3d regions for the Co + TiO_2/Ag and Co/PET + TiO_2/Ag fibers are presented in Figs. 4 and 5, respectively. The comparison of chemical composition between untreated and modified Co and Co/PET fabrics derived from high resolution scans are summarized in Table 1. In general, Co fibers comprise of α-cellulose (88–96.5 %) and non-cellulosic components like waxes, pectin, proteins and inorganic matter. Pectic substances and waxes are located in the cuticle layer and primary wall that are considered as outer layers of Co fiber (Chung et al. 2004). Cellulose is polysaccharide consisting of linear chains of β (1–4) D-glucose units. Therefore, C–OH, O–C–O and C–O–C groups detected in C1s signal of investigated Co fibers can be attributed to cellulose (Fig. 3a). It is suggested that the O–C–O groups partially originate from pectic substances (Chung et al. 2004; Topalovic et al. 2007; Tourrette et al. 2009). Additional peak corresponding to C–C/C–H groups is also recorded. This peak can be assigned to cotton waxes. Namely, waxes are mixtures of

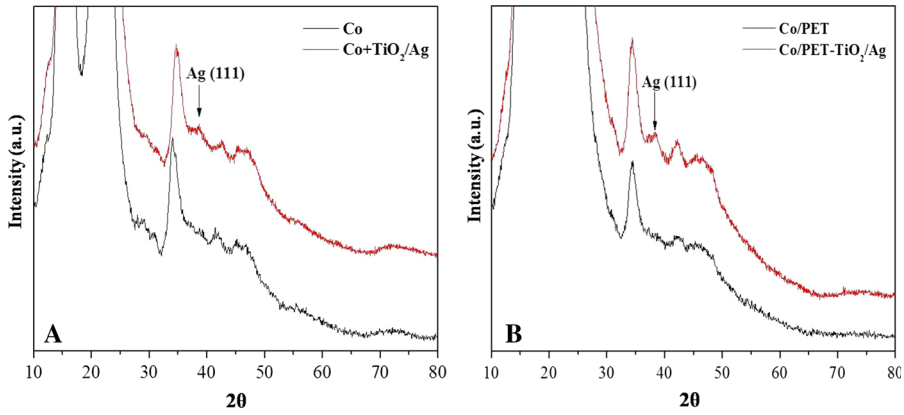

Fig. 2 XRD patterns of **a** Co and Co + TiO_2/Ag samples and **b** Co/PET and Co/PET + TiO_2/Ag samples

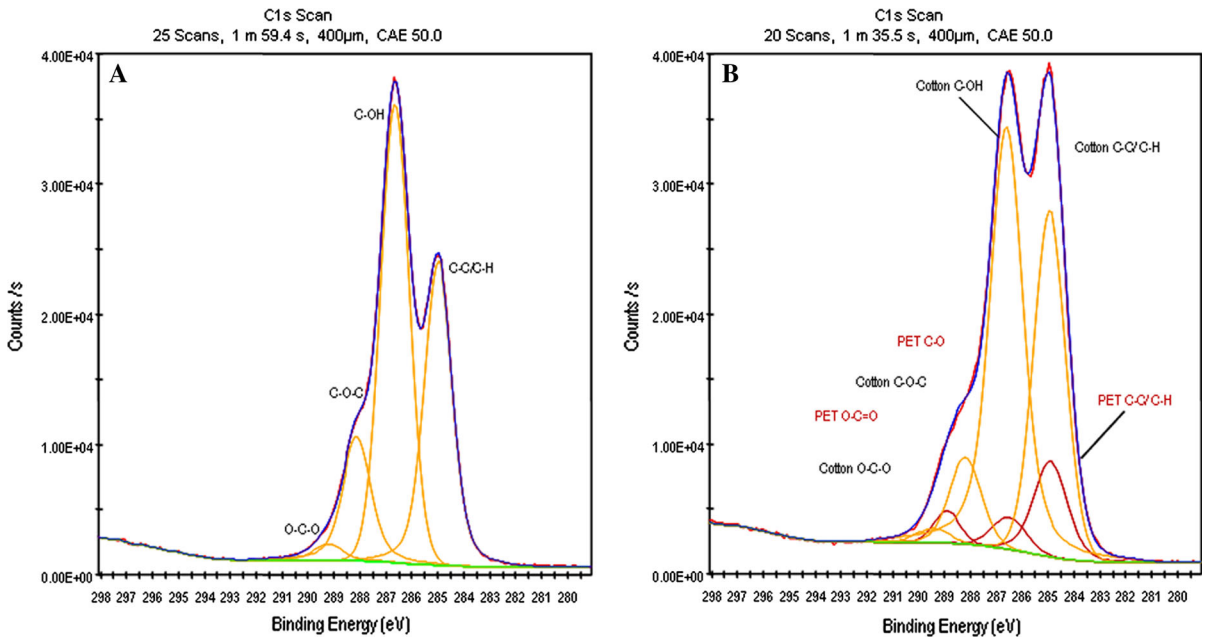

Fig. 3 High resolution XPS C1s spectra of **a** Co and **b** Co/PET fabrics

hydrocarbons, alcohols, esters and free acids with long alkyl chains (Chung et al. 2004). Hence, they contain considerable amount of carbon atoms without oxygen neighbors (Fras et al. 2005). On the other hand, the carbon is commonly absorbed on the surface of polymers, metals and metal oxides when exposed to air (Johansson 2007). Thus, it is assumed that some of recorded C–C/C–H groups are due to adventitious contamination. The intensity of C–C/C–H peaks is affected by the laboratory conditions during the sample preparation and the spectrophotometer itself (Kontturi et al. 2003).

Additional O–C=O, C–O and C–C/C–H groups originating from PET were recorded in the C1s signal of the Co/PET blend (Fig. 3b). The peak at 284.7 eV is assigned to carbon atoms bound to carbon or hydrogen in benzene ring (C–C, C–H). The peak at 286.45 eV corresponds to methylene carbons single bonded to oxygen (C–O) while the peak at 288.91 eV is attributed to ester carbon atoms (O–C=O).

Table 1, Figs. 4a and 5a reveal that the amount of carbon functional groups on the Co + TiO_2/Ag and Co/PET + TiO_2/Ag fabrics decreased after photoreduction of Ag^+-ions. In addition to organic O, clear

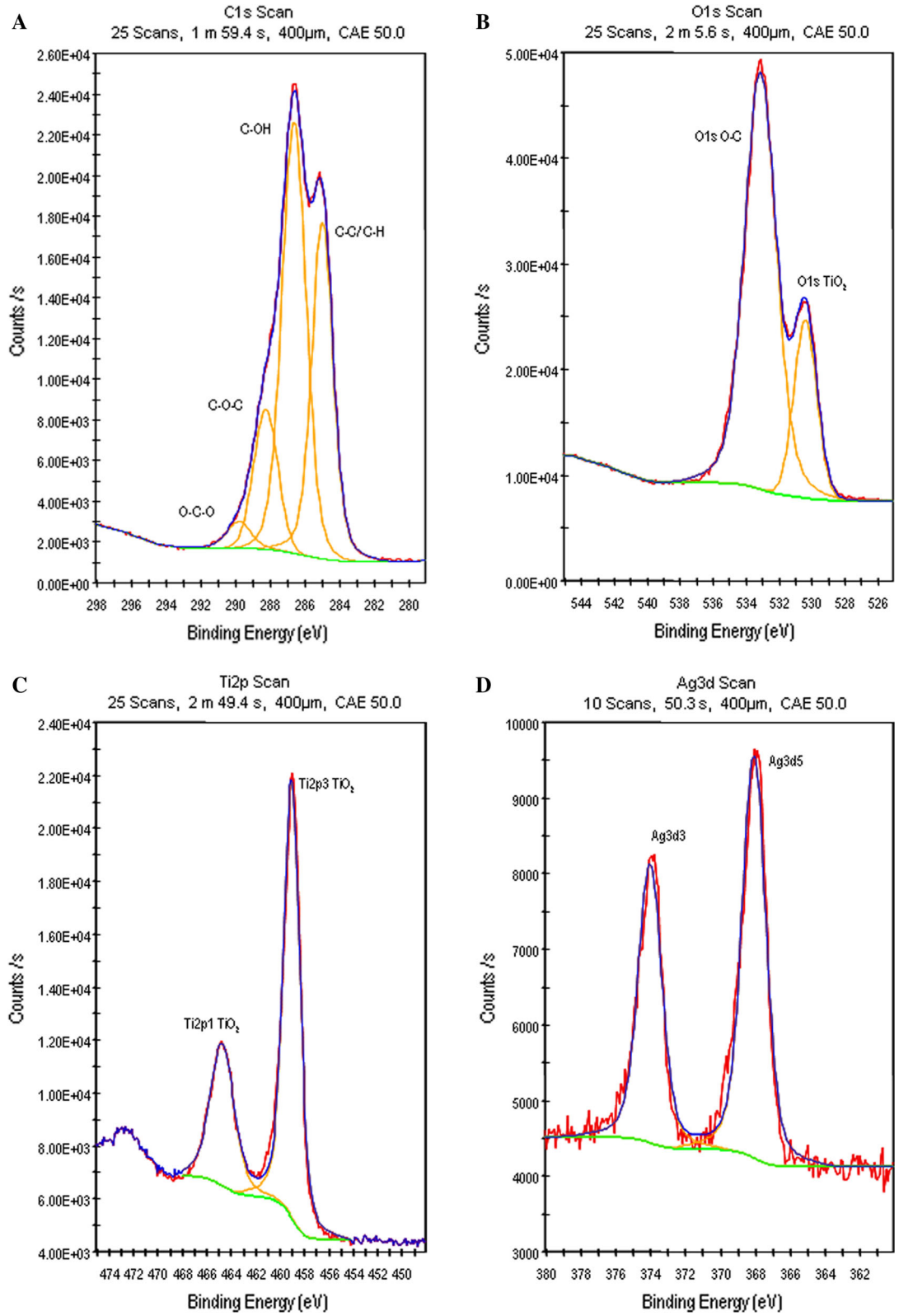

Fig. 4 High resolution XPS **a** C1s, **b** O1s, **c** Ti2p and **d** Ag3d spectra of the Co + TiO_2/Ag fabric

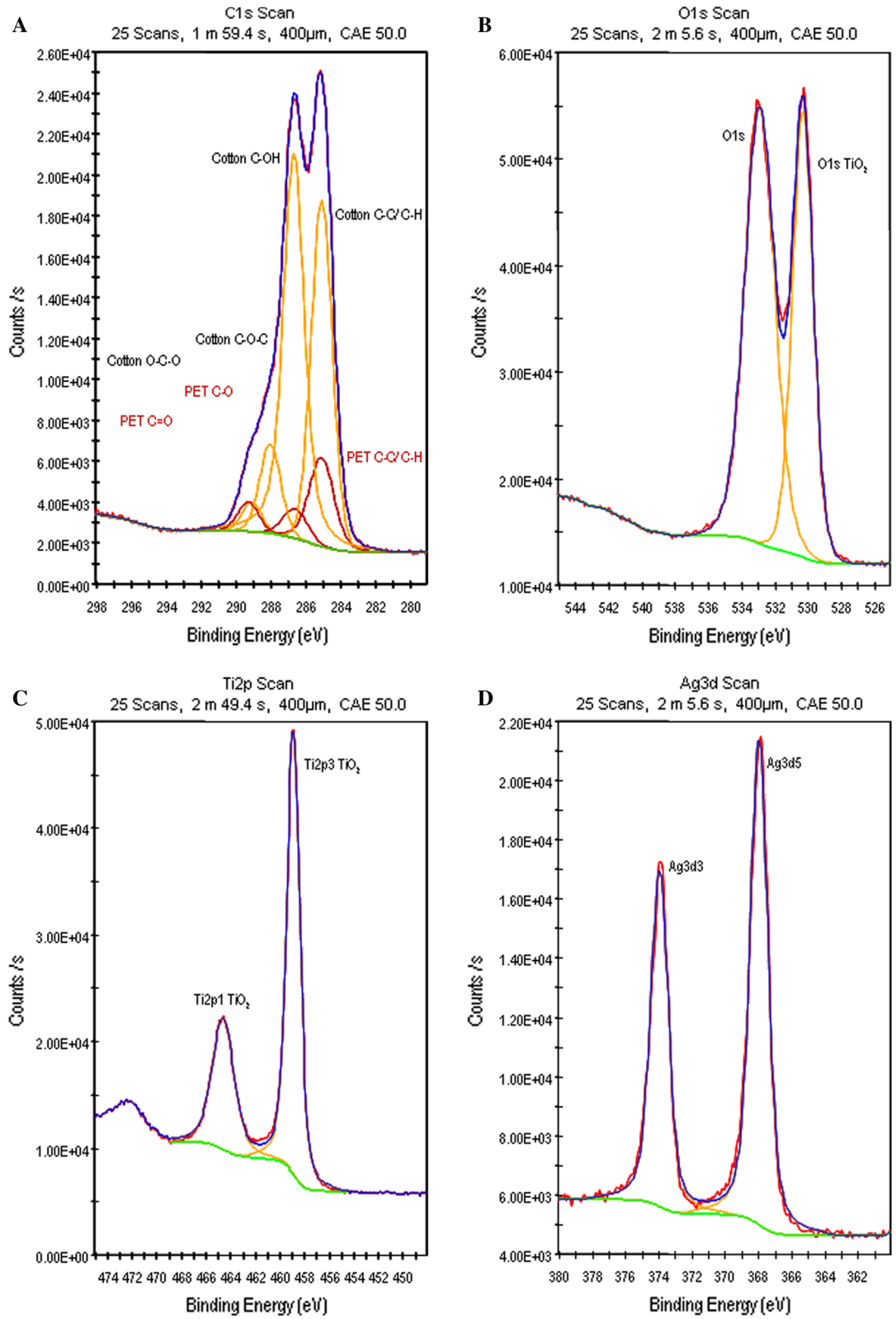

Fig. 5 High resolution XPS **a** C1s, **b** O1s, **c** Ti2p and **d** Ag3d spectra of the Co/PET + TiO_2/Ag fabric

Table 1 Comparison of chemical composition of Co, Co/PET, Co + TiO_2/Ag and Co/PET + TiO_2/Ag fabrics derived from high resolution XPS spectra

	Atom %			
	Co	Co/PET	Co + TiO_2/Ag	Co/PET + TiO_2/Ag
O (organic)	35.94	34.32	30.13	27.49
O (TiO_2)	0.00	0.00	11.39	13.71
C1s C–OH (Co)	31.74	28.66	24.26	21.27
C1s C–C/C–H (Co)	21.65	14.25	17.21	11.05
C1s C–O–C (Co)	8.58	8.44	7.61	6.13
C1s O–C–O (Co)	1.62	0.85	1.56	1.43
C1s C–C/C–H (PET)	0.00	8.08	0.00	6.30
C1s C–O (PET)	0.00	2.55	0.00	1.99
C1s C=O (PET)	0.00	1.99	0.00	1.55
Ti (TiO_2)	0.00	0.00	6.32	7.14
N	0.25	0.48	0.74	0.71
Si	0.23	0.38	0.31	0.12
Ag	0.00	0.00	0.49	1.10

peak corresponding to O in TiO_2 in O1s spectra of the Co + TiO_2/Ag and Co/PET + TiO_2/Ag fabrics confirm the presence of TiO_2 NPs (see Figs. 4b, 5b). The Ti $2p_{1/2}$ and Ti $2p_{3/2}$ spin-orbital splitting electrons are located at binding energies of 464.2 and 458.6 eV, respectively (see Figs. 4c, 5c). The results from Table 1 indicate that within experimental error (±10 % of atomic percent value) Ti content on the surface of Co + TiO_2/Ag and Co/PET + TiO_2/Ag fabrics is almost the same.

The high resolution XPS spectra of the Co + TiO_2/Ag and Co + TiO_2/Ag fibers surface in the region of binding energies related to Ag3d core-electrons are shown in Figs. 4d and 5d, respectively. The accurate determination of the oxidation state of silver deposited on the fabrics is not a simple task due to variation of particle size and electrostatic charging (Yuranova et al. 2003). Reference value of binding energy for metallic Ag is 368.2 eV^2. In the current study, the position of $Ag3d_{5/2}$ peak is shifted towards lower binding energies (367.7 eV) which is close to the binding energy assigned to Ag_2O (367.8 eV) (Yuranova et al. 2003). This finding disagrees with the results of the XRD analysis, i.e. the presence of Ag in metallic form. Keeping in mind the surface sensitivity of XPS, it could be supposed that detected peak relates to layer of Ag_2O generated on the surface of Ag NPs. This hypothesis relies on the fact that though the incident X-rays penetrate deep into the sample, the emitted photoelectrons have a strong interaction with the solid. This attenuation length is typically in the range of 1–10 nm, depending on the surface composition and the binding energy of the emitted photoelectron. For the $Ag3d_{5/2}$ orbital, the attenuation length is such that the signal arises from the top 4 nm of the surface, with the majority of the signal being from the outermost 1.5 nm. Taking into account that the average dimension of the TiO_2/Ag NPs was approximately 70 nm, it is very likely that XPS provides only information corresponding to outer surface of particles.

In addition, data in Table 1 demonstrated that larger amount of Ag has been found on the surface of Co/PET + TiO_2/Ag fabric (1.1 %) compared to Co + TiO_2/Ag fabric (0.49 %). However, AAS measurements indicated that larger amount of Ag has been fabricated on the surface of the Co + TiO_2/Ag fabric. Namely, one gram of Co + TiO_2/Ag and Co/PET + TiO_2/Ag fabrics contains 290 and 165 μg of Ag, respectively. This discrepancy between XPS and AAS results can be attributed to uneven deposition of TiO_2/Ag NPs that was confirmed by XPS mapping. It should be also kept in mind that AAS gives the information on total amount of fabricated Ag whereas XPS is confined to the thin surface layer of Co and Co/PET fibers.

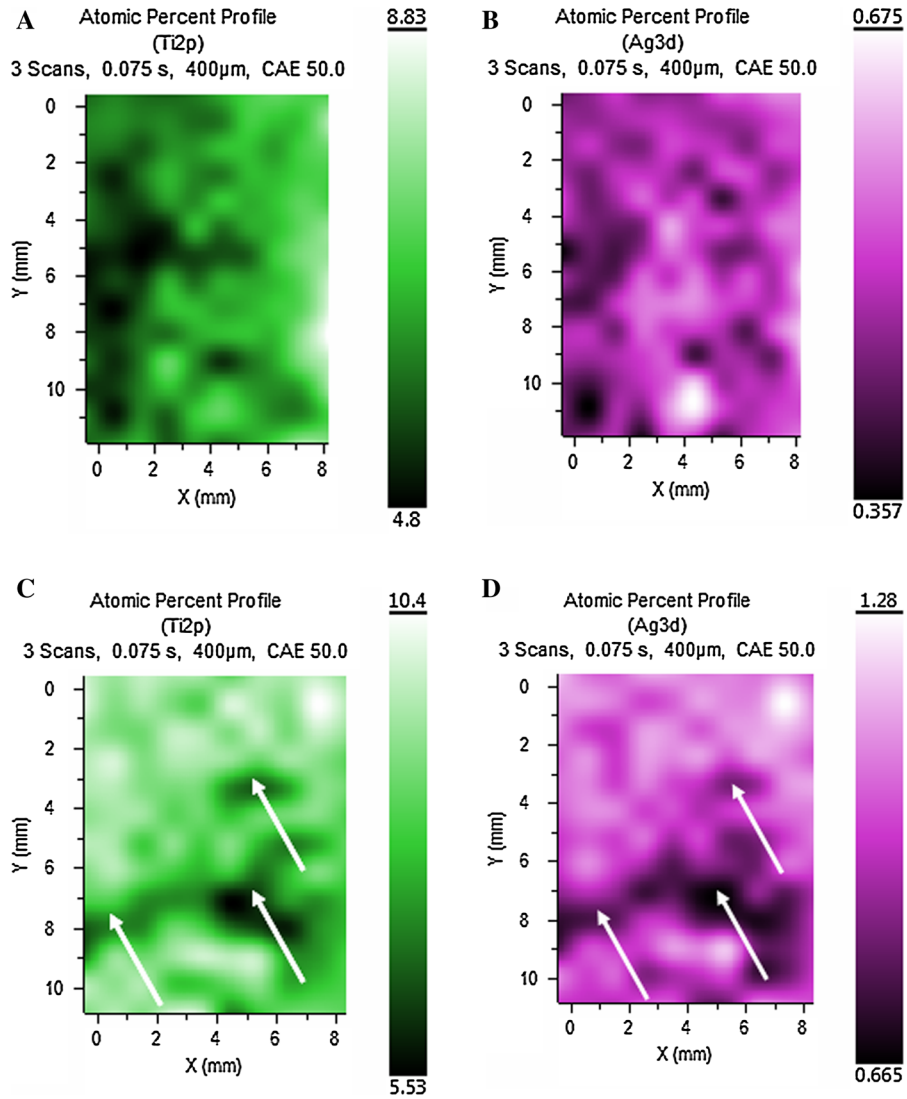

Fig. 6 TiO_2 mapping of the surfaces of the **a** Co + TiO_2/Ag and **c** Co/PET + TiO_2/Ag fabrics; **b** Ag mapping of the surfaces of the Co + TiO_2/Ag and **d** Co/PET + TiO_2/Ag fabrics

7.755 × 11.473 mm^2 area of the Co + TiO_2/Ag fabric and 7.882 × 10.390 mm^2 area of the Co/PET + TiO_2/Ag fabric were mapped in steps of 850 µm and C1s, O1s, Ti2p and Ag3d signals were measured at each point. The number of data points for these samples was 130. For this discussion atomic percent profiles for Ti2p and Ag3d signals are particularly important and they are shown in Fig. 6. Presented images clearly indicate that quite uneven distribution of TiO_2/Ag NPs on the surface of Co and especially Co/PET fabrics has been obtained. Evidently, there are some areas that are uncoated and they are higher in carbon content (not shown). The amount of Ti on investigated samples is roughly half of the maximum and approximately 2 % lower than average (Table 1). Further, it could be noticed that areas with smaller amounts of Ti also contain smaller amount of Ag and vice versa. This was particularly prominent on the Co/PET sample and such areas are marked with arrows in Fig. 6c, d. According to these results it could be suggested that larger amount of deposited TiO_2 NPs facilitates the photoreduction of Ag^+-ions and eventually larger quantities of metallic Ag is formed. The EDX analysis of scanned single TiO_2/Ag nanoparticle deposited on the Co and Co/PET fibers also proved that peaks corresponding to both Ti and Ag regularly appeared in the spectra (Fig. 7). Therefore, this confirms that our original idea has been realized and Ag was fabricated on deposited TiO_2 NPs.

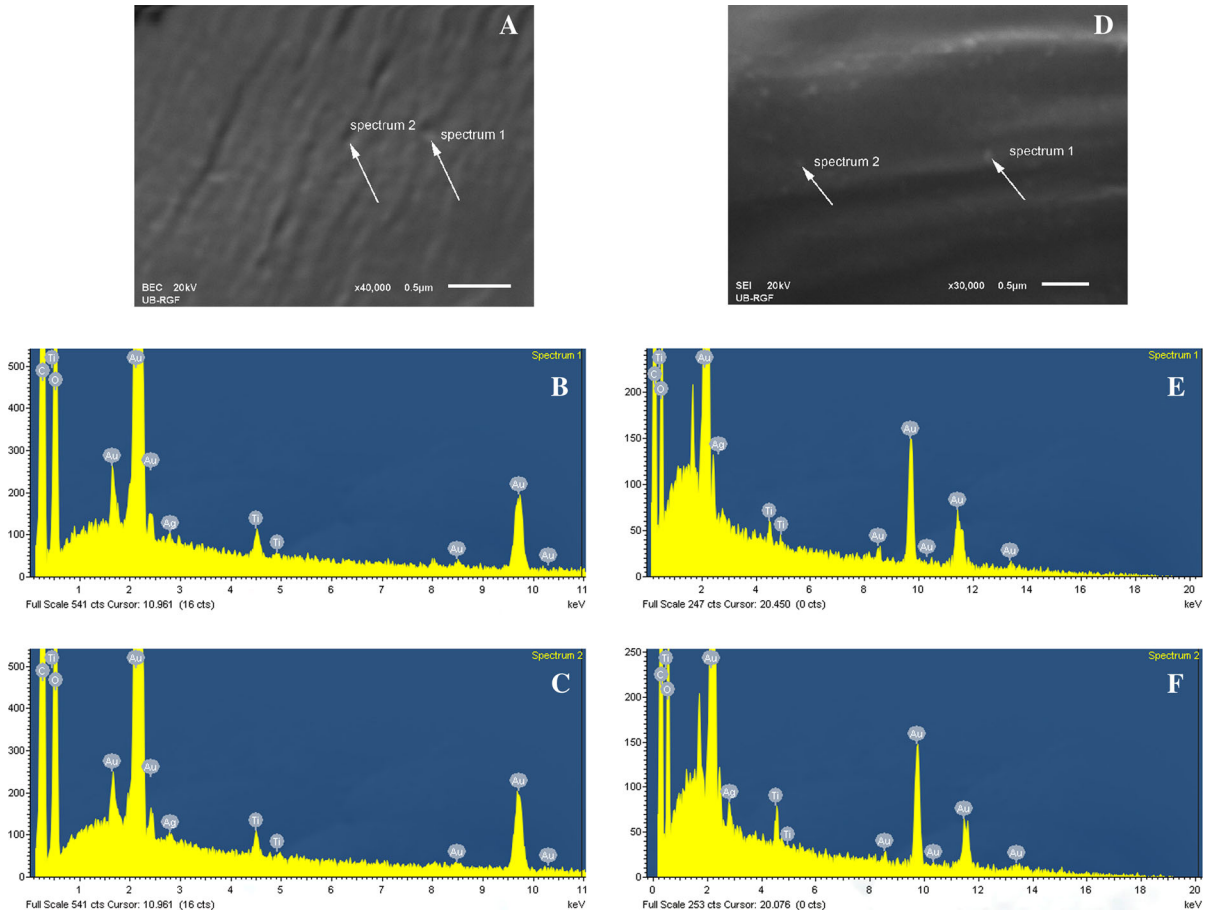

Fig. 7 SEM images and EDX spectra of **a–c** Co + TiO_2/Ag and **d–f** Co/PET + TiO_2/Ag fibers

Interaction between silver and alanine modified TiO_2 NPs

FTIR spectra were recorded with an aim to get information on a possible interaction between silver and alanine modified TiO_2 NPs. The vibrational spectra of pure alanine, alanine after binding to Ag^+-ions, after adsorption on the surface of TiO_2 NPs, and after adsorption on TiO_2 NPs and binding to Ag^+-ions are shown in Fig. 8. The main bands and their assignment in free alanine are as follows: asymmetric and symmetric stretching vibration of OCO^- group at 1,592 ($\nu_{as}OCO^-$), 1,414 ($\nu_{as}OCO^-$) (Bellamy 1975), and 1,361 (ν_sOCO^-) cm^{-1}; bending vibrations of NH_3^+ group at 1,622 ($\delta_{as}NH_3^+$), and doublet at 1,518/1,507 ($\delta_sNH_3^+$) cm^{-1}, rocking vibrations of NH_3^+ group at 1,237, 1,153 and 1,115 (ρNH_3^+) cm^{-1}; bending vibrations of CH_3 groups at 1,454 ($\delta_{as}CH_3$) and 1,411 (δ_sCH_3) cm^{-1} and bending vibrations of CH bond at 1,307 (δCH) cm^{-1} (Garcia et al. 2008).

Few changes in vibrational spectrum of Ala/Ag were observed after binding of Ag^+-ions to alanine. The decrease in intensity of asymmetric stretching vibration of OCO^- group at 1,414 cm^{-1} and the appearance of new band at 1,383 cm^{-1} indicated an interaction of silver and OCO^- group from alanine, i.e. unidentate binding of silver and carboxyl group (Socrates 2001). A new band at 1,274 cm^{-1} in Ala/Ag spectrum is suggested to be an effect of deprotonation of alanine amino groups and this change is followed by decrease in intensity of rocking vibration (ρNH_3^+) at 1,237 cm^{-1} and symmetric bending vibration (δ_s-NH_3^+) at 1,518 cm^{-1} (Rosado et al. 1997). This effect is also responsible for the appearance of new band at 1,195 cm^{-1} characteristic for the presence of NH_2 group (Rajh et al. 1998). Finally, a weak band in the

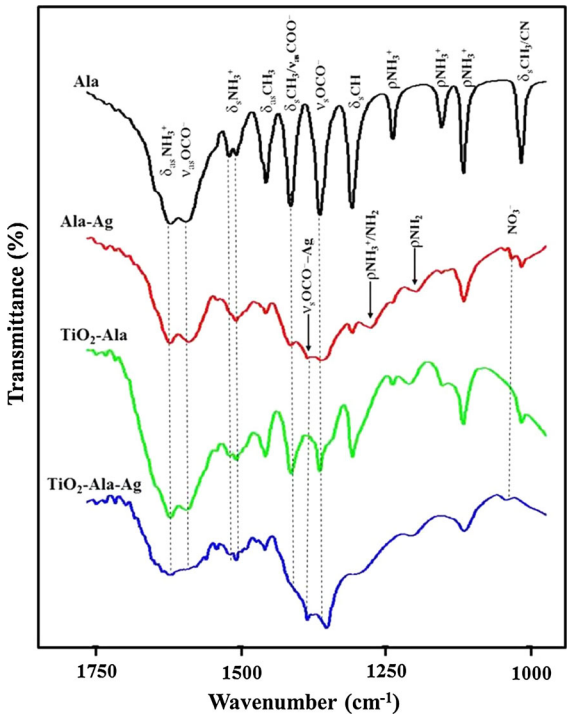

Fig. 8 FTIR spectra of pure alanine, alanine after binding to Ag^+-ions, alanine after adsorption on the surface of TiO_2 NPs and alanine after adsorption on TiO_2 NPs and binding to Ag^+-ions

Ala/Ag vibrational spectrum at 1,037 cm^{-1} indicates the presence of NO_3^- as a residue of precursor (Socrates 2001).

A slight decrease of intensity of bands at 1,592 and 1,362 cm^{-1}, which correspond to asymmetric and symmetric stretching vibrations of COO^- (νOCO^-) group in vibrational spectrum of alanine after adsorption on the surface of TiO_2 NPs was observed. Vibrational spectrum of alanine after adsorption on the surface of TiO_2 NPs and binding to Ag^+-ions reveals further decrease of intensity of band at 1,592 cm^{-1} ($\nu_{as}OCO^-$) and almost complete disappearance of the band at 1,414 ($\nu_{as}OCO^-$) cm^{-1}. The band that appeared in Ala/Ag vibrational spectrum still exists at 1,383 cm^{-1}, suggesting that the interaction between TiO_2, alanine and silver has been established. In other words, carboxyl group of alanine bridges surface titanium and silver ions in the structure which enhances the symmetrical stretching. This assumption is in agreement with finding of Rajh et al. (1998). They explained the binding of copper ions to the surface of TiO_2 NPs through carboxyl group of alanine followed by appearance of new band assigned to C–O band at 1,380 cm^{-1} order of 1.5. A possible binding structure of silver to the surface of alanine modified TiO_2 NPs is shown in Fig. 9.

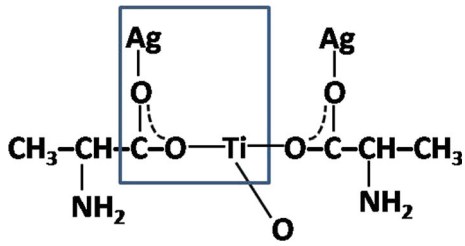

Fig. 9 Possible binding structure of silver to the surface alanine modified TiO_2 NPs

Antibacterial activity of cotton and cotton/PET fabrics impregnated with TiO_2/Ag NPs

Antibacterial activity of Co and Co/PET fabrics impregnated with TiO_2/Ag NPs was tested in the dark against bacteria *E. coli* and *S. aureus*. The results from Tables 2 and 3 demonstrate that maximum bacteria reduction was reached with both fabrics. Although the amount of fabricated Ag on the Co fabric was by 35 % smaller compared to the Co fabric modified in accordance with original procedure, maximum bacteria reduction was obtained and it was preserved after ten washing cycles. The Co/PET + TiO_2/Ag fabric exhibited almost the same behavior but the reduction of *S. aureus* colonies decreased after ten washing cycles. Despite this slight decrease, antibacterial efficiency against *S. aureus* was considered as an excellent.

Washing fastness of cotton and cotton/PET fabrics impregnated with TiO_2/Ag NPs

Although excellent antibacterial activity of Co and Co/PET fabrics impregnated with TiO_2/Ag NPs even after ten washing cycles was obtained, significant release of silver occurred during washing (Table 4). Considerable amount of silver leached out from the fabrics particularly in the first three washing cycles. Afterwards, smaller but still significant amounts of silver were released from the fabrics. Silver release was more than three times larger in the case of Co + TiO_2/Ag fabric. In spite of observed release about 50 % of

Table 2 Antibacterial activity of Co fabric impregnated with TiO_2/Ag NPs

Sample	Bacteria	Number of bacterial colonies (CFU)	R (%)
Before washing			
Control Co	*E. coli*	1.9×10^5	
Co + TiO_2/Ag		40	99.9
Control Co	*S. aureus*	1.8×10^5	
Co + TiO_2/Ag		<10	99.9
After 10 washing cycles			
Control Co	*E. coli*	1.1×10^4	
Co + TiO_2/Ag		<10	99.9
Control Co	*S. aureus*	1.4×10^5	
Co + TiO_2/Ag		60	99.9

Table 3 Antibacterial activity of Co/PET fabric impregnated with TiO_2/Ag NPs

Sample	Bacteria	Number of bacterial colonies (CFU)	R (%)
Before washing			
Control Co/PET	*E. coli*	1.2×10^5	
Co/PET + TiO_2/Ag		<10	99.9
Control Co/PET	*S. aureus*	1.9×10^5	
Co/PET + TiO_2/Ag		25	99.9
After 10 washing cycles			
Control Co/PET	*E. coli*	1.2×10^5	
Co/PET + TiO_2/Ag		<10	99.9
Control Co/PET	*S. aureus*	1.9×10^5	
Co/PET + TiO_2/Ag		360	99.8

initial Ag amount remained on the Co fabric after washing ensuring maximum bacterial reduction.

Perspiration fastness of cotton and cotton/PET fabrics impregnated with TiO_2/Ag NPs

The study on the perspiration fastness of the Co + TiO_2/Ag and Co/PET + TiO_2/Ag fabrics pointed out that release of silver also occurred in both acidic (pH = 5.5) and alkaline (pH = 8.0) artificial sweat. 12.15 and 17.53 μg of silver leached out from one gram of the Co + TiO_2/Ag fabric in acidic and alkaline sweat, respectively. Similar behavior was noticed on the Co/PET + TiO_2/Ag fabric: 14.53 and 18.13 μg of silver were released under the same conditions. Evidently, larger release of silver occurred in alkaline sweat. Such trend was already reported in literature (Kulthong et al. 2010).

Table 4 Silver release during washing of Co + TiO_2/Ag and Co/PET + TiO_2/Ag fabrics

Washing cycles	Release of silver (μg/g) Co + TiO_2/Ag fabric	Release of silver (μg/g) Co/PET + TiO_2/Ag fabric
1	24.4 ± 6.7	15.4 ± 2.3
2	25.6 ± 3.2	6.9 ± 4.1
3	20.4 ± 2.8	4.3 ± 2.2
4	12.8 ± 2.4	4.6 ± 1.5
5	15.4 ± 6.2	4.4 ± 2.9
6	11.2 ± 2.0	5.0 ± 2.0
7	19.9 ± 4.8	3.9 ± 0.8
8	10.0 ± 4.0	1.9 ± 0.5
9	9.1 ± 2.9	1.3 ± 0.2
10	10.8 ± 0.7	2.4 ± 0.4

UV protection of cotton and cotton/PET fabrics impregnated with TiO_2/Ag NPs

The presence of TiO_2/Ag NPs on the surface of the Co and Co/PET fabrics produced additional effect. UV protective properties of investigated fabrics were significantly improved after fabrication of TiO_2/Ag NPs. The recommendation is to supply garment with excellent to maximum UPF rating (Xin et al. 2004). The coating of both fabrics with TiO_2/Ag NPs resulted in maximum UPF rating (50+). UPF values and UPF ratings of Co and Co/PET fabrics before and after washing are given in Table 5. UPF values of the Co + TiO_2/Ag fabric decreased after five and ten washing cycles likely due to detachment of NPs during washing, UPF rating of 50+ was preserved even after ten washing cycles. In the case of Co/PET fabric, UPF values slightly increased after washing. The longer the washing, the higher the UPF values. Such behavior was already reported in literature and it was attributed to rearrangement of NPs on the surface of fabrics during washing (Paul et al. 2010). However, taking into account that PET fibers are components of the studied blend as well as that such trend was not found in the case of Co + TiO_2/Ag fabric, we believe that this slight improvement appears as a result of fabric

Table 5 UV protection properties of Co and Co/PET fabrics impregnated with TiO_2/Ag NPs

Sample	UPF[a]	UPF rating
Co	7.2 ± 0.6	5
Co + TiO_2	62.4 ± 1.3	50+
Co + TiO_2/Ag	111.9 ± 1.8	50+
Co + TiO_2/Ag (after 5 washing cycles)	81.6 ± 0.6	50+
Co + TiO_2/Ag (after 10 washing cycles)	74.0 ± 1.7	50+
Co/PET	36.7 ± 2.7	30
Co/PET + TiO_2	70.7 ± 3.1	50+
Co/PET + TiO_2/Ag	114.2 ± 16.5	50+
Co/PET + TiO_2/Ag (after 5 washing cycles)	124.4 ± 10.6	50+
Co/PET + TiO_2/Ag (after 10 washing cycles)	134.8 ± 10.6	50+

[a] UPF-UV protection factor

shrinking during washing which additionally contribute to blocking of UV light (Paul et al. 2010).

Summary

In situ photoreduction of Ag^+-ions with TiO_2 nanoparticles deposited on cotton and cotton/PET fabrics in the presence of alanine and methyl alcohol resulted in generation of TiO_2/Ag nanoparticles. The existence of TiO_2/Ag nanoparticles on the surface of both fabrics was confirmed by SEM, EDX, XRD, XPS and AAS analyses. The formation of TiO_2/Ag nanoparticles was proved by EDX while the results of FTIR analysis suggested that carboxyl group of amino acid alanine likely bridges surface titanium and silver ions establishing the interaction between them.

The fabrics impregnated with TiO_2/Ag nanoparticles provided excellent antibacterial activity against Gram-negative bacterium *E. coli* and Gram-positive bacterium *S. aureus* which was preserved after ten washing cycles. In spite of satisfactory washing fastness, the leaching of silver during washing was prominent particularly from the cotton fabric. Silver was also released from both fabrics in the artificial sweat, in particular in alkaline conditions. The presence of TiO_2 nanoparticles provided maximum level of UV protection.

Acknowledgments The financial support for this work was provided by the Ministry of Education, Science and Technological Development of Republic of Serbia (Projects No. 45020 and 172056). The work is done under the umbrella of COST Action MP1106. We gratefully acknowledge Dr. B. Jokić (University of Belgrade, Serbia) for providing FESEM measurements.

References

Bellamy LJ (1975) The infrared spectra of complex molecules. Chapman and Hall, London

Breitenkamp M, Henglein A, Lilie J (1976) Mechanism of the reduction of lead ions in aqueous solution (a pulse radiolysis study). Ber Bunsenges Phys Chem 80:973–979

Chung C, Lee M, Choe EK (2004) Characterization of cotton fabric scouring by FTIR ATR spectroscopy. Carbohydr Polym 58:417–420

Daoud WA, Xin JH, Zhang YH (2005) Surface functionalization of cellulose fibers and their combined bactericidal activities. Surf Sci 599:69–75

El-Shishtawy RM, Asiri AM, Abdelwahed NA, Al-Otaibi MM (2011) In situ production of silver nanoparticle on cotton fabric and its antimicrobial evaluation. Cellulose 18:75–82

Fras L, Johansson LS, Stenius P, Laine J, Stana-Kleinschek K, Ribitsch V (2005) Analysis of the oxidation of cellulose fibres by titration and XPS. Colloid Surf A 260:101–108

Garcia AR, de Barros RB, Loureno JP, Ilharco LM (2008) The infrared spectrum of solid L-alanine: influence of pH-induced structural changes. J Phys Chem A 112:8280–8287

Gorenšek M, Recelj P (2007) Nanosilver functionalized cotton fabric. Text Res J 77:138–146

Gorjanc M, Kovač F, Gorenšek M (2012) The influence of vat dyeing on the adsorption of synthesized colloidal silver onto cotton fabrics. Text Res J 82:62–69

Ilić V, Šaponjić Z, Vodnik V, Potkonjak B, Jovančić P, Nedeljković J, Radetić M (2009) The influence of silver content on antimicrobial activity and color of cotton fabrics functionalized with Ag nanoparticles. Carbohydr Polym 78:564–569

Johansson K (2007) Plasma modification of natural cellulosic fibres. In: Shishoo R (ed) Plasma technologies for textiles. Woodhead Publishing in textiles, Cambridge, pp 251–260

Kelly FM, Johnston JH (2011) Colored and functional silver nanoparticle—wool fiber composites. ACS Appl Mater Interface 3:1083–1092

Kontturi E, Thüne PC, Niemantsverdriet JW (2003) Novel method for preparing cellulose model surfaces by spin coating. Polymer 44:3621–3625

Krklješ AN, Marinović-Cincović M, Kačarević-Popović ZM, Nedeljković JM (2007) Radiolytic synthesis and characterization of Ag-PVA nanocomposites. Eur Polym J 43:2171–2176

Kulthong K, Srisung S, Boonpavanitchakul K, Kangwansupamonkon W, Maniratanachote R (2010) Determination of silver nanoparticle release from antibacterial fabrics into artificial sweat. Part Fibre Toxicol 7:1–8

Lee JH, Jeong SH (2005) Bacteriostasis and skin innoxiousness of nanosize silver colloids on textile fabrics. Text Res J 75:551–556

Lee HJ, Yeo SY, Jeong SH (2003) Antibacterial effect of nanosized silver colloidal solution on textile fabrics. J Mater Sci 38:2199–2204

Messaoud M, Chadeau E, Brunon C, Ballet T, Rappenne L, Roussel F, Leonard D, Oulahal N, Langlet M (2010) Photocatalytic generation of silver nanoparticles and application to the antibacterial functionalization of textile fabrics. J Photochem Photobiol A 215:147–156

Mihailović D, Šaponjić Z, Radoičić M, Radetić T, Jovančić P, Nedeljković J, Radetić M (2010) Functionalization of polyester fabrics with alginates and TiO_2 nanoparticles. Carbohydr Polym 79:526–532

Mihailović D, Šaponjić Z, Molina R, Radoičić M, Esquena J, Jovančić P, Nedeljković J, Radetić M (2011) Multifunctional properties of polyester fabrics modified by corona discharge/air RF plasma and colloidal TiO_2 nanoparticles. Polym Compos 32:390–397

Milošević M, Radoičić M, Šaponjić Z, Nunney T, Marković D, Nedeljković J, Radetić M (2013a) In situ generation of Ag nanoparticles on polyester fabrics by photoreduction using TiO_2 nanoparticles. J Mater Sci 48:5447–5455

Milošević M, Radoičić M, Šaponjić Z, Marković D, Nedeljković J, Radetić M (2013b) In situ generation of Ag nanoparticles by photoreduction with TiO_2 nanoparticles deposited onto cotton fabric. Proc EUROMAT 2013, European Congress and Exhibition on Advanced Materials and Processes, Symposium, C3I: nano-powder development by advanced techniques, Sevilla, CD book of abstracts C3I-P-TU-PS1-11

Nam S, Condon BD (2014) Internally dispersed synthesis of uniform silver nanoparticles via in situ reduction of $[Ag(NH_3)_2]^+$ along natural microfibrillar substructures of cotton fiber. Cellulose. doi:10.007/s10570-014-0270-y

Nogami G, Kennedy JH (1989) Investigation of "current doubling" mechanism of organic compounds by the rotating ring disk electrode technique. J Electrochem Soc 136:2583–2588

Paul R, Bautista L, De la Varga M, Botet JM, Casals E, Puntes V, Marsal F (2010) Nano-cotton fabrics with high ultraviolet protection. Text Res J 80:454–462

Pohle D, Damm C, Neuhof J, Rösch A, Münstedt H (2007) Antimicrobial properties of orthopaedic textiles after in situ deposition of silver nanoparticles. Polym Polym Compos 15:357–363

Radetić M (2013) Functionalization of textile materials with silver nanoparticles. J Mater Sci 48:95–107

Radetić M, Ilić V, Vodnik V, Dimitrijević S, Jovančić P, Šaponjić Z, Nedeljković J (2008) Antibacterial effect of silver nanoparticles deposited on corona treated polyester and polyamide fabrics. J Polym Adv Technol 19:1816–1821

Rajh T, Ostafin A, Mićić OI, Tiede DM, Thurnauer MC (1996) Surface modification of small particle TiO_2 colloids with cysteine for enhanced photochemical reduction: an EPR study. J Phys Chem 100:4538–4545

Rajh T, Nedeljković J, Chen LX, Tiede DM, Thurnauer MC (1998) Photoreduction of copper on TiO_2 nanoparticles modified with polydentate ligands. J Adv Oxid Technol 3:292–298

Rosado MTS, Duarte MLRS, Fausto R (1997) Vibrational spectra (FT-IR, Raman and MI-IR) of α- and β-alanine. J Mol Struct 410–411:343–348

Socrates G (2001) Infrared and Raman characteristic group frequencies. Wiley, England

Stockhausen VK, Henglein A (1971) Pulsradiolytsche Untersuchung des Mechanismus der Oxidation and Autooxidation von Formaldehyd in Waessriger Loesung. Ber Bunsenges Phys Chem 75:833–840

Tang B, Kaur J, Sun L, Wang X (2013) Multifunctionalization of cotton through in situ green synthesis of silver nanoparticles. Cellulose 20:3053–3065

Thompson RC (1984) Oxidation of peroxotitanium (IV) by chlorine and cerium (IV) in acidic perchlorate solution. Inorg Chem 23:1794–1798

Topalovic T, Nierstrasz VA, Bautista L, Jocic D, Navarro A, Warmoeskerken MMCG (2007) XPS and contact angle of cotton surface oxidation by catalytic bleaching. Colloid Surf A 296:76–85

Tourrette O, De Geyter N, Jocic D, Morent R, Warmoeskerken MMCG, Leys C (2009) Incorporation of poly(N-isopropylacrylamide)/chitosan microgel onto plasma functionalized cotton fibre surface. Colloid Surf A 352:126–135

Vigneshwaran N, Kathe AA, Varadarajan PV, Nachane PP, Balasubramanya RH (2007) Functional finishing of cotton fabrics using silver nanoparticles. J Nanosci Nanotechnol 7:1893–1897

Xin JH, Daoud WA, Kong YY (2004) A new approach to UV-blocking treatment for cotton fabrics. Text Res J 74:97–100

Yin C, Li J, Xu Q, Peng Q, Liu Y, Shen X (2007) Chemical modification of cotton cellulose in supercritical carbon dioxide: synthesis and characterization of cellulose carbamate. Carbohydr Polym 67:147–154

Yuranova T, Rincon AG, Bozzi A, Parra S, Pulgarin C, Albers P, Kiwi J (2003) Antibacterial textiles prepared by RF-plasma and vacuum-UV, mediated deposition of silver. J Photochem Photobiol A 161:27–34

Zhong-Ai H, Yao-Xian W, Yu-Long X, Yu-Ying Y, Zi-Yu Z, Hong-Ying W (2010) Ag nanowires and its application as electrode materials in electrochemical capacitor. J Appl Electrochem 40:341–344